DFT-assisted XANES simulations to discriminate different monomeric CuII species in CHA catalysts

(Article begins on next page)

07 January 2023

DFT-assisted XANES simulations to discriminate different monomeric Cu^{II} species in CHA catalysts

I. A. Pankin[1,2*], E. Borfecchia[2,3,4], A. Martini[1,6], K. A. Lomachenko[5], C. Lamberti[1,6], A. V. Soldatov[1]

[1] International Research Institute "Smart Materials", Southern Federal University, 344090 Rostov-on-Don (Russia)
[2] Department of Chemistry and INSTM Reference Center, University of Turin, 10125 Turin (Italy)
[3] Center for Materials Science and Nanotechnology (SMN), Department of Chemistry, University of Oslo, 0315 Oslo (Norway)
[4] Haldor Topsøe A/S, Haldor Topsøes Allé 1, 2800 Kongens Lyngby (Denmark)
[5] European Synchrotron Radiation Facility, 38043 Grenoble Cedex 9 (France)
[6] Department of Physics and INSTM Reference Center, University of Turin, 10125 Turin (Italy)
*e-mail: ipankin@unito.it

Abstract

Herein, we present Cu K-edge XANES (X-ray Absorption Near Edge Structure) simulations for different framework interacting Z-Cu^{II} species proposed to form as an active site after high-temperature activation in Cu-exchanged chabazite zeolites, representing promising materials for selective catalytic reduction of NO$_x$ in the presence of ammonia and direct conversion methane to methanol. We critically compare the simulated spectra to previously collected data for an O$_2$-activated Cu-chabazite sample. Density of states (DOS) calculations allow us to get more insights in describing the nature of XANES features observed in the simulated spectra. To demonstrate the potential of the method, we finally explore the impact of systematic variations of selected structural parameters on the theoretical XANES features.

Keywords

XANES simulations, DFT, DOS, Cu-chabazite, zeolites, selective catalytic reduction, partial oxidation

1. Introduction

During the last decade, zeolites extensively used in heterogeneous catalysis as their inner cavities offer a restricted environment providing high selectivity for a wide range of reactions (Smit and Maesen, 2008). Transition metal-exchanged zeolites provide a most efficient way to decompose harmful NO$_x$ in the presence of ammonia molecules being a promising catalyst for SCR (selective catalytic reduction) application (Groothaert et al., 2003). The same materials nowadays are also intensively studied for the selective oxidation of methane to methanol, so called (MTM) (Groothaert et al., 2005).

Recently Cu-exchanged zeolites have been exhaustively studied by means of in-situ and operando UV-Vis, FTIR and Cu K-edge XAS spectroscopic techniques (Giordanino et al., 2014; Giordanino et al., 2013) reflecting a big variety of different Cu sites and their different population which is shown to be sensitive to different activation and reaction conditions (Borfecchia et al., 2015; Lomachenko et al., 2016) as well as topology and composition (Martini et al., 2017) (Cu:Al and Si:Al ratios) of the catalysts.

Although the recent results obtained thanks to the unique structural/electronic sensitivity of X-ray absorption spectroscopy (XAS) assisted by Density Functional Theory (DFT) modelling (Borfecchia et al., 2015) and implementation of advanced XAS data analysis approaches such as MCR-ALS (Multivariate Curve Resolution- Alternating Least-Squares method) (Martini et al., 2018; Martini et al., 2017), the formation of diffent framework-interacting Cu^{II} species in the activated state is still under discussion. This issue is exhaustively investigated on the DFT-level in a numbers of previous studies (Ipek et al., 2017; Paolucci et al., 2016; Sushkevich et al., 2017).

In our recent study (Pappas et al., 2017) we have presented a two possible routes of formation for framework interacting Z-Cu$^{II}_x$O$_y$ species formation: from a self-reduced ZCu^{I} by interaction with an oxygen molecules which can result to the formation of monomeric super-oxo sites, or due to the internal pathways preferably resulting to the formation of dimeric framework-interacting species. In both mechanisms, framework interactiong Z-Cu^{II}OH species is supposed to be a starting point (before the formation of self reduced ZCu^{I} sites) which implies also quite abundant population of this species in the activated sample.

Reffering to our previous investigation (Martini et al., 2017) for He-activated Cu-CHA (hereinafter CHA is used as reduction from "chabazite" and specify zeolite topology) samples with a different composition, this CuOH moieties has been reported to be hosted in the 1Al 8MR site.

In a present work we have considered different Cu^{II} species, including the above described Z-Cu^{II}OH and two super-oxo Z-Cu^{II}O$_2$ models in side-on and end-on binding mode incorporated in 8MR of Cu-CHA in the proximity of 1Al sites. Being more focused on Cu K-edge XANES (X-ray Absorption Near Edge Structure) simulations, we are aimed to figure out some fingerprint features in the simulated spectra making allowing

discrimination among different monomeric Cu^{II} sites in the activated state. We also report density of state (DOS) calculations in order to shed light on the nature of XANES features and correlate it with the electronic structure of the respecive Cu-species. Finally as an example for the four-fold coordinated side-on model we have demonstrated how the shape of XANES spectra could be affected by a structural modifications also tracking changes in a XANES simulated spectrum upon a possible side-on → end-on transformation.

This work could be also considered as a starting point for the further attempts to disciminate possible monomeric and dimeric species. It also demonstrates the accessibility of XANES simulations by finite difference full potential approach, to catch the spectroscopic fingerprints linked to different structural motifs.

2. Theoretical approaches

Spin-polarized DFT simulations were performed using plane wave pseudopotential approach as implemented in the VASP 5.3 package (Kresse and Furthmuller, 1996). Cell volume and atomic positions have been subsequently used as variable parameters in the geometry relaxation procedure. PBE pseudopotentials (Kresse and Joubert, 1999) were implemented for all atomic sites. Conjugate gradients iteration scheme was employed for energy minimization procedure. Block Davidson scheme was employed for electronic SCF cycles convergence. The energy convergence criteria for the electronic cycles has been set as 10^{-5} eV. A kinetic energy cutoff of 450 eV and 400 eV was used to restrict plane wave basis set for volume and atomic positions relaxation, respectively. 2x2x2 K-point Γ-centered meshes automatically generated by means of Monokhorts-Pack scheme were implemented for sampling of Brillouin zone in reciprocal space. DFT-D3 scheme of Grimme et. al.(Grimme et al., 2010) as implemented in VASP 5.3 has been employed to take into account a possible Van der Waals interaction.

XANES simulations has been performed by using full potential finite difference approach as implemented in FDMNES code (Joly, 2001) which recently was significantly accelerated by the implementation of sparse solver method (Guda et al., 2015). The Finite Difference Method (FDM) is attractive for calculations of the photoelectron wave function up to 100-200 eV above the absorption edge. It avoids in a simple way the muffin tin approximation (Slater, 1937) used in most of the software for XAS simulations, for example in all the multiple scattering theory (MST) based codes. The density of electronic states has been also calculated in FDMNES code.

3. Results and discussion

The selected three models of Cu^{II} sites have been incorporated into pre-optimized 36 T-sites unit cell of Cu-CHA taking into account as an initial guess the structural parameters obtained in previous literature, using cluster (Borfecchia et al., 2015; Martini et al., 2017) and periodic approaches (Falsig et al., 2016). Afterwards volume optimization has been performed. Considering that the concentration of Cu ions incorporated into zeolite is relatively small and should not affect the lattice parameters, this step, in principle, could be ignored. Nevertheless, since the XANES is very sensitive to even small changes in bond lengths in proximity of absorbing atoms, we have considered a possible local perturbation in the unit cell volume when the Cu^{II} sites are included. To obtain a final geometry, atomic position relaxation has been performed keeping the unit cell volume fixed to the optimized value. Fig. 1 (a,b,c) report a fragments of optimized models.

The results of Cu K-edge XANES simulations are reported in Fig. 1(d) in comparison with an experimental XAS data acquired at BM26A beamline of ESRF (Grenoble, France) for Cu-CHA (0.5;12) sample in a steady-state conditions after the activation. Activation has been performed in oxygen atmosphere by heating the cell from RT to 500 ºC with the ramp rate of 5 ºC/min. The XANES spectrum simulated for side-on super-oxo model provides a better agreement being the only one model reflecting all the three features (referred to as A, B and C at Fig. 1(d)) observed in experimental curve and demonstrating a less developed rising-edge feature A with respect to three-coordinated end-on and "CuOH" models.

Taking into account previously published results (Martini et al., 2017)it is evident that in a real case a mixture of at least two different Cu-species exists in the activated Cu-CHA. Thus, the comparison of the simulated spectra with a principle component XANES curves could be more correct. Fig. 1(e) demonstrates that the XANES spectra simulated for four-fold coordinated side-on model exhibit better agreement with a principal component curve PC4 (Martini et al., 2018), derived from MCR-ALS analysis of a HERFD-XANES dataset collected at ID26 beamline for Cu-CHA (0.5;12) sample during O_2 activation, which is characterized by more sharp "step like" rising-edge feature A with respect to the conventional XANES data collected on BM23 (black curve).

In order to achieve a better understanding of the nature of the ~~of the~~ above reported features in the simulated spectra, the density of electronic state (DOS) has been calculated. Fig. 3 reports the DOS calculation results

obtained for Z-Cu^{II}O$_2$ model in a side-on configuration and for Z-Cu^{II}OH model supposed to be a precursor for further formation of super-oxo species (Pappas et al., 2017).

For the side-on model, the rising edge feature A arises due the preferential hybridization of Cu p-states with p-states of framework oxygens (O$_{fw}$) rather that extra-framework oxygens (O$_{ef}$). However, both framework and extra-framework oxygen p-states contribute similarly to the intensity of shoulder B. Moreover, a broad "white line" peak C is observed in the convoluted spectra reflecting two features referred to as C^1 and C^2.
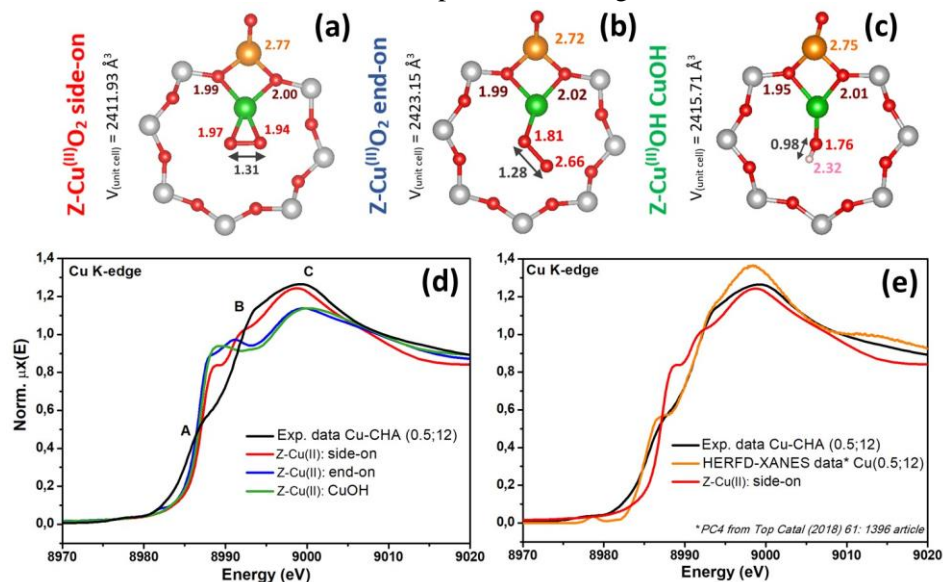
Fig. 1. (a,b,c) Different Cu-oxo species incorporated into 8MR of Cu-CHA with an optimized volume and distances (reported in Å). The color code: grey, red, orange, green and pink spheres corresponds to Si, O, Al, Cu and H atoms, respectively. (d) XANES Cu K-edge simulations results for the above reported geometries in comparison with experimental XANES acquired for O$_2$ activated Cu-CHA (0.5;12). (e) XANES Cu K-edge simulations for side-on model in comparison with experimental spectra (ascribed in part (d) of the figure) and HERFD-XANES principal component data reported in work (Martini et al., 2018). Simulated XANES has been adjusted in the energy position by the shift of + 6.73 eV.

before the convolution. These transitions most likely originate from the hybridizations of p-, d- states of Cu and p-states of Al, which exhibit significantly higher density of unoccupied states in this energy region with respect to p- states of both O$_{fw}$ and O$_{ef}$. For Z-Cu^{II}OH the situation is less unambiguous since the rising-edge shoulder A in the convoluted spectra reflected a series of sharps peaks very close to each other in energy deriving from the mixing of p-states of Cu with a p states of Al, as well as both framework and extra-framework oxygens. The "white line" broad peak B as in the case of the side-on model is mostly originated by the mixing of Cu p- and Al p-states showing higher availability of unoccupied states in this energy region with respect to O$_{fw}$ and O$_{ef}$. The lower-intensity feature C (not reflected in the convoluted spectra) is also predominantly provided by the hybridization of Cu and Al p-states.
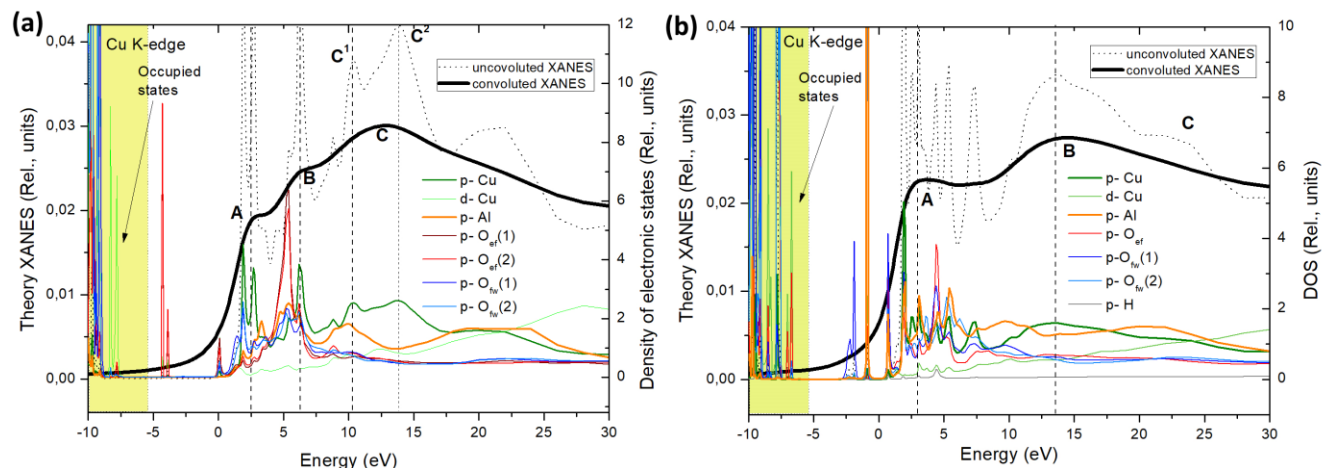
Fig. 2 Cu K-edge XANES simulated spectra before and after convolution in comparison with a partial density of states of the atoms in the nearest proximity of absorbing Cu atom calculated for (a) Z-Cu^{II}O$_2$ side-on and (b) Z-Cu^{II}OH optimized models. The theoretical XANES spectra are represented in the relative energy scale. The calculated Fermi energy level

equal to -6.13 eV and -5.83 eV for Z-Cu^{II}O$_2$ side-on and Z-Cu^{II}OH models, respectively, determine the border rectangular yellow area in the low energy part of the plots separating the range of occupied states.

Finally, we have performed a series of XANES simulations for a side-on geometry with varied structural parameters to explore the simulations sensitivity to possible modifications in the investigated Cu^{II} species. As it has been shown in Fig. 1(e,d), the spectra simulated for side-on model seems to be a little bit contracted showing a lower energy distance between rising-edge feature A and "white line" maximum C with respect to experimental data. Fig, 4(a) reports a simulated XANES for side-on with a shortened Cu-O$_{ef}$ distances and fixed O$_{ef}$-Cu-O$_{ef}$ angle which results in the gradual shifts to the higher energy range of the peak B and C position (with respect to A) in accordance with Natoli's rule (A. Bianconi, 1983) and could improve this disagreement with experimental data.
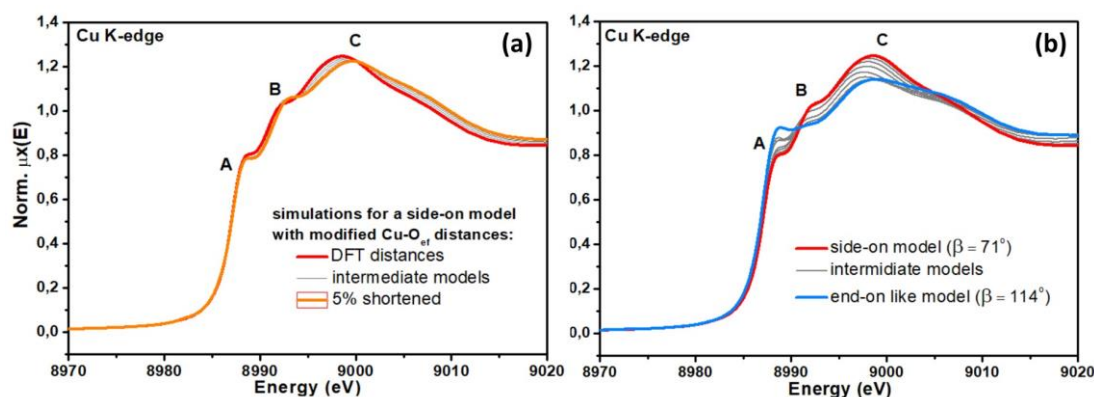
Fig. 3 (a) Cu K-edge XANES simulations for a side-on models with a shortened Cu-O$_{ef}$ distances (b) Evolution of Cu K-edge XANES simulated spectra upon the structural modifications starting from a side-on geometry and ending with a "end-on like" geometry.

Figure 4(b) reports the simulation results to mimic a possible transformation from side-on to "end-on like" structural configuration by cleaving one of the Cu-O$_{ef}$ bonds and gradual increasing of the Cu-O$_{ef(1)}$-O$_{ef(2)}$ angle β starting from the side-on geometry (Cu-O$_{ef(1)}$ = 1.94 Å, Cu-$_{Oef(2)}$ = 1.97 Å and β=71°) and ending up with "end-on like" configuration (Cu-O$_{ef(1)}$ = 1.81 Å, Cu-$_{Oef(2)}$ = 2.67 Å and β=114°). With respect to the distance modifications reported in Fig. 4(a), the simulated spectra evidently show much more drastic evolution characterized by a more developed rising-edge feature A, accompanied by significant damping of white line peak intensity as well as modifications of its general shape (resulting in end-on like white line shape) and finally by the disappearing of the shoulder B clearly observed for the several starting models. These results exhibit the potential of XANES simulations to discriminate not only different configurations of different Cu-oxo species, but also to catch their structural variations providing additional information for EXAFS quantitative analysis which is almost not reflecting angular variations.

4. Conclusions

In this work we employed full potential DFT-assisted Cu K-edge XANES simulations for different monomeric Cu^{II} species incorporated into 1Al 8MR sites of Cu-exchanged chabazite. The simulation results showed that four-fold super-oxo Z-Cu^{II}O$_2$ in a side-on binding mode configuration provides a better fit of experimental data collected for O$_2$ activated Cu-CHA (0.5;12) being possibly a more abundant site in the activated state. Nonetheless, further studies will be required to better understand the complexity of Cu-speciation in the O$_2$-activated state, also considering three-fold coordinated models with more similar Cu-O$_{fw}$ and Cu-O$_{ef}$ distances in accordance with an EXAFS analysis (not reported in this contribution). Analysis of partial density of electronic states allowed us to assign different features of the simulated spectra with an electronic configuration. The evolution of the simulated spectrum for a side-on model under systematic modifications of selected structural parameters exhibit the potential of these approaches to discriminate not only different Cu-sites but also fine modifications in their geometry.

References

A. Bianconi, M.D.A., A. Gargano, C.R. Natoli, 1983 EXAFS and Near Edge Structure I. Springer Series in Chemical Physics, pp. 57-61.

Borfecchia, E., Lomachenko, K.A., Giordanino, F., Falsig, H., Beato, P., Soldatov, A.V., Bordiga, S., Lamberti, C., 2015. Revisiting the nature of Cu sites in the activated Cu-SSZ-13 catalyst for SCR reaction. Chem. Sci. 6, 548-563.

Falsig, H., Vennestrøm, P.N.R., Moses, P.G., Janssens, T.V.W., 2016. Activation of Oxygen and NO in NH3-SCR over Cu-CHA Catalysts Evaluated by Density Functional Theory. Topics in Catalysis 59, 861-865.

Giordanino, F., Borfecchia, E., Lomachenko, K.A., Lazzarini, A., Agostini, G., Gallo, E., Soldatov, A.V., Beato, P., Bordiga, S., Lamberti, C., 2014. Interaction of NH3 with Cu-SSZ-13 Catalyst: A Complementary FTIR, XANES, and XES Study. J. Phys. Chem. Lett. 5, 1552-1559.

Giordanino, F., Vennestrom, P.N.R., Lundegaard, L.F., Stappen, F.N., Mossin, S., Beato, P., Bordiga, S., Lamberti, C., 2013. Characterization of Cu-exchanged SSZ-13: a comparative FTIR, UV-Vis, and EPR study with Cu-ZSM-5 and Cu-beta with similar Si/Al and Cu/Al ratios. Dalton Trans. 42, 12741-12761.

Grimme, S., Antony, J., Ehrlich, S., Krieg, H., 2010. A consistent and accurate ab initio parametrization of density functional dispersion correction (DFT-D) for the 94 elements H-Pu. J. Chem. Phys. 132.

Groothaert, M.H., Smeets, P.J., Sels, B.F., Jacobs, P.A., Schoonheydt, R.A., 2005. Selective oxidation of methane by the bis(mu-oxo)dicopper core stabilized on ZSM-5 and mordenite zeolites. J. Am. Chem. Soc. 127, 1394-1395.

Groothaert, M.H., van Bokhoven, J.A., Battiston, A.A., Weckhuysen, B.M., Schoonheydt, R.A., 2003. Bis(mu-oxo)dicopper in Cu-ZSM-5 and its role in the decomposition of NO: A combined in situ XAFS, UV-Vis-Near-IR, and kinetic study. J. Am. Chem. Soc. 125, 7629-7640.

Guda, S.A., Guda, A.A., Soldatov, M.A., Lomachenko, K.A., Bugaev, A.L., Lamberti, C., Gawelda, W., Bressler, C., Smolentsev, G., Soldatov, A.V., Joly, Y., 2015. Optimized Finite Difference Method for the Full-Potential XANES Simulations: Application to Molecular Adsorption Geometries in MOFs and Metal-Ligand Intersystem Crossing Transients. J. Chem. Theory Comput. 11, 4512-4521.

Ipek, B., Wulfers, M.J., Kim, H., Goltl, F., Hermans, I., Smith, J.P., Booksh, K.S., Brown, C.M., Lobo, R.F., 2017. Formation of Cu2O2 (2+) and Cu2O (2+) toward C-H Bond Activation in Cu-SSZ-13 and Cu-SSZ-39. ACS Catal. 7, 4291-4303.

Joly, Y., 2001. X-ray absorption near-edge structure calculations beyond the muffin-tin approximation. Phys. Rev. B 63.

Kresse, G., Furthmuller, J., 1996. Efficiency of ab-initio total energy calculations for metals and semiconductors using a plane-wave basis set. Comput. Mater. Sci. 6, 15-50.

Kresse, G., Joubert, D., 1999. From ultrasoft pseudopotentials to the projector augmented-wave method. Phys. Rev. B 59, 1758-1775.

Lomachenko, K.A., Borfecchia, E., Negri, C., Berlier, G., Lamberti, C., Beato, P., Falsig, H., Bordiga, S., 2016. The Cu-CHA deNO(x) Catalyst in Action: Temperature-Dependent NH3-Assisted Selective Catalytic Reduction Monitored by Operando XAS and XES. J. Am. Chem. Soc. 138, 12025-12028.

Martini, A., Alladio, E., Borfecchia, E., 2018. Determining Cu–Speciation in the Cu–CHA Zeolite Catalyst: The Potential of Multivariate Curve Resolution Analysis of In Situ XAS Data. Topics in Catalysis 61, 1396-1407.

Martini, A., Borfecchia, E., Lomachenko, K.A., Pankin, I.A., Negri, C., Berlier, G., Beato, P., Falsig, H., Bordiga, S., Lamberti, C., 2017. Composition-driven Cu-speciation and reducibility in Cu-CHA zeolite catalysts: a multivariate XAS/FTIR approach to complexity. Chem. Sci. 8, 6836-6851.

Paolucci, C., Parekh, A.A., Khurana, I., Di Iorio, J.R., Li, H., Caballero, J.D.A., Shih, A.J., Anggara, T., Delgass, W.N., Miller, J.T., Ribeiro, F.H., Gounder, R., Schneider, W.F., 2016. Catalysis in a Cage: Condition-Dependent Speciation and Dynamics of Exchanged Cu Cations in SSZ-13 Zeolites. J. Am. Chem. Soc. 138, 6028-6048.

Pappas, D.K., Borfecchia, E., Dyballa, M., Pankin, I.A., Lomachenko, K.A., Martini, A., Signorile, M., Teketel, S., Arstad, B., Berlier, G., Lamberti, C., Bordiga, S., Olsbye, U., Lillerud, K.P., Svelle, S., Beato, P., 2017. Methane to Methanol: Structure Activity Relationships for Cu-CHA. J. Am. Chem. Soc. 139, 14961-14975.

Slater, J.C., 1937. Wave Functions in a Periodic Potential. Physical Review 51, 846-851.

Smit, B., Maesen, T.L.M., 2008. Towards a molecular understanding of shape selectivity. Nature 451, 671-678.

Sushkevich, V.L., Palagin, D., Ranocchiari, M., van Bokhoven, J.A., 2017. Selective anaerobic oxidation of methane enables direct synthesis of methanol. Science 356, 523-+.